

PHYSICAL REVIEW B

CONDENSED MATTER

THIRD SERIES, VOLUME 34, NUMBER 12

15 DECEMBER 1986

Iron on palladium (111) studied with photoemission, low-energy electron diffraction, and Auger-electron spectroscopy

C. Binns and C. Norris

Physics Department, Leicester University, Leicester LE1 7RH, United Kingdom

Gwyn P. Williams

National Synchrotron Light Source, Brookhaven National Laboratory, Upton, New York 11973

M. G. Barthes

Laboratoire de Physico Chimie des Surfaces, Ecole Nationale Supérieure de Chimie Physique, Université Pierre et Marie Curie, 75005, Paris, France

H. A. Padmore

Science and Engineering Research Council, Daresbury Laboratory, Daresbury, Cheshire WA4 4AD, United Kingdom

(Received 8 November 1985; revised manuscript received 8 September 1986)

Ultrathin Fe films on Pd(111) have been characterized by low-energy electron diffraction and Auger-electron spectroscopy and their electronic and magnetic properties studied by photoelectron spectroscopy using synchrotron radiation. By controlling the substrate temperatures during deposition it has been possible to grow islanded multilayer films, flat monolayer platelets, and flat bilayer platelets. Evidence is presented indicating that a flat Fe monolayer on Pd (111) is paramagnetic with a local moment of $1.2\mu_B$. Small coverages in the second layers appear to induce ferromagnetic order. At coverages around two monolayers the films appear to pass through an antiferromagnetic phase.

I. INTRODUCTION

The magnetization of transition metals in contact with nonmagnetic materials is an active area of study. Perturbation of the electronic orbitals due to hybridization and structural modification associated with epitaxial growth should lead to significant changes in magnetic behavior. Thus, paramagnetism has been observed in nickel monolayers on copper¹ and amorphous $Pb_{15}Bi_{25}$ alloy² substrates. Tersoff and Falicov³ calculated the local moment of nickel atoms at the (100) surface of a bulk crystal coated with a copper monolayer and found it reduced to about half of the bulk nickel value. Recent measurements have confirmed this behavior for the Ni(111)/Cu(111) interface.⁴

The iron-palladium system is of particular interest in view of the tendency for palladium to become magnetically "active" in the presence of magnetic ions.^{5,6} Using the anomalous Hall effect (AHE), Bergmann⁷ reported that iron adsorbed on polycrystalline palladium exhibits a paramagnetic to ferromagnetic transition as the coverage is increased beyond 0.5 monolayers. The magnetic state is, however, sensitive to local order, and in an earlier report⁸ it was suggested that magnetic order is a conse-

quence of iron atoms in the second adsorbate layer.

We describe here a more complete study of the behavior of iron on the palladium (111) surface. Low-energy electron diffraction (LEED) and Auger-electron spectroscopy (AES) are used to demonstrate that both flat monolayer and bilayer islands are formed after annealing different coverages. We have investigated the local magnetic moment of the iron atoms via the multiple splitting of the iron 3s core level. Photoelectron spectroscopy (PES) of the valence bands has also been used.

II. EXPERIMENT

The LEED, AES, and the valence-band photoemission measurements were made with the ADES 400 spectrometer on beam line VI at the Science and Engineering Research Council's Daresbury laboratory. The pressure in the chamber was normally 1×10^{-10} mbar and never rose above 3×10^{-10} mbar during iron evaporation. The valence-band photoemission spectra were recorded at a photon energy of 120 eV and with a combined (monochromator and analyzer) energy resolution of 0.4 eV. With the relatively large light spot incident on the sample the angular resolution was degraded to about $\pm 10^\circ$ and thus the re-

sults are more representative of angle integrated photoemission spectra.

Core-level photomission spectra were obtained on beam line U14 of the VUV storage ring at the National Synchrotron Light Source facility, Brookhaven, New York with an ultrahigh vacuum chamber, equipped with LEED optics and a cylindrical mirror analyzer. The pressure rose from a base value of 2×10^{-10} mbar and to 8×10^{-10} mbar during iron evaporation. The spectra were recorded at 160 eV photon energy and a combined energy resolution of 1.1 eV.

The palladium (111) sample was cleaned by repeated cycles of argon-ion sputtering and annealing until no contaminant Auger peaks could be detected. The iron vapor source consisted of an alumina knudsen cell surrounded by a water-cooled shield.

III. RESULTS

A. AES results

Iron overlayers on Pd(111) do not grow in a simple manner and the growth mode changes significantly with relatively small changes in substrate temperature. Since the magnetic state of iron depends critically on local atomic coordination, it is clear that a detailed understanding of the growth mode as a function of temperature is required before interpreting the photoemission results.

Figure 1 shows an Auger signal versus evaporation time ($A_S - t$) plot for iron deposited on palladium at room temperature. The smooth featureless curves for both the iron and palladium signals are indicative of a growth mode

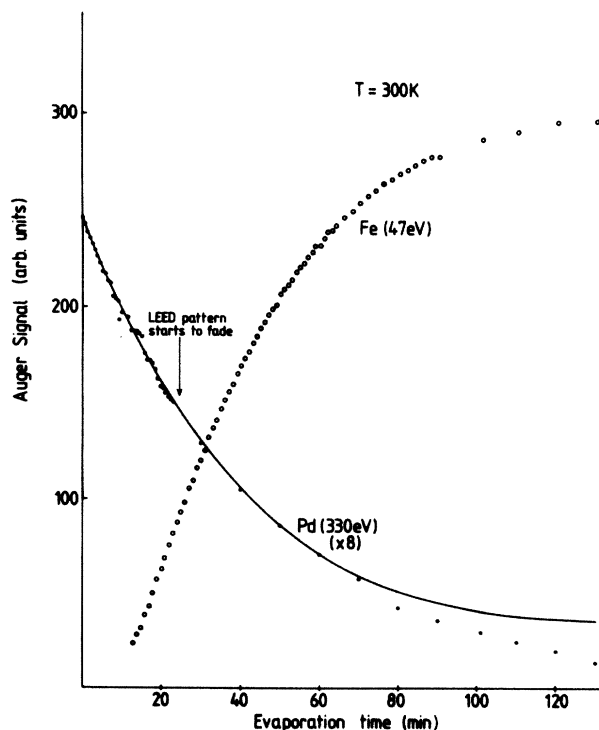


FIG. 1. $A_S - t$ plot of the Fe MVV and Pd LVV Auger signals for Fe deposited at room temperature.

which is not simple layer-by-layer (Frank van der Merwe). The LEED pattern remains $p(1 \times 1)$ over the range of the plot but begins to deteriorate after the substrate signal has been attenuated to 60% of its original value. We can estimate the evaporation rate of iron from the evaporator to within $\pm 50\%$, and thus the slope of the curves determines the overlayer growth to be in the simultaneous multilayer (SM) mode. Formation of bulk crystallites would also give a smooth curve but with much smaller slope. The SM growth mode involves the development of the n th layer before the $(n-1)$ th layer is complete and has been described by Barthes and Rolland.⁹ The solid line in Fig. 1 shows the predicted variation of the palladium MVV Auger signal with iron as predicted by the equations given in Ref. 9. A parameter in the calculation is the scattering length for palladium MVV (330 eV) Auger electrons in iron. This was measured from the high-temperature $A_S - t$ plot, in which breaks can be distinguished, to be 3.52 monolayers (see below). The calculated curve follows the experimental results closely to high coverages. We believe the departure from the data at the highest coverages is due to a change in the growth mode of the overlayer. This, however, is not relevant to the present study which concentrates on the monolayer and bilayer structures. Cooling the substrate to 100 K during evaporation of the iron does not change the growth mode as expected since SM growth relies on a short diffusion length of the overlayer.

We know from Ref. 8 that the overlayer structure changes significantly if the substrate temperature is raised to 450 K so we repeated the $A_S - t$ plot with the substrate maintained at this temperature. The result for the palladium signal is shown in Fig. 2, and this time two breaks can be distinguished. We attribute the most prominent break at $t = 74$ min to the completion of a bilayer of iron. To interpret this break as the formation of a monolayer or trilayer would imply an unrealistic value of the scattering length of palladium MVV Auger electrons. The formation of stable bilayers on substrates at sufficiently high temperatures has been predicted by Stoyanov and Markov¹⁰ and has been observed in the case of nickel segregation on a Cu(111) surface.⁹ Following the theory of Stoyanov and Markov¹⁰ we can also explain the first break in Fig. 2 at $t = 18$ min. They showed that a monolayer island becomes metastable when the number of atoms in it reaches a critical value given by [for deposition on an fcc(111) face]:

$$N_{12} = (0.96/\phi = 1.23)^2.$$

Here $\phi = 1 - \psi'/\psi$ is the so-called "adhesion parameter," where ψ' is the work necessary to separate a deposit atom from a substrate atom and ψ is the work necessary to separate two deposited atoms. If the temperature is sufficiently high to overcome the activation barrier involved, monolayer islands will undergo a transition to bilayer islands by detachment of atoms from the edges and the formation of a new layer on top of the first. We attribute the first kink in Fig. 2 to this transition as the average monolayer island size exceeds N_{12} and further growth occurs by the increase in size of bilayer platelets. We cannot find

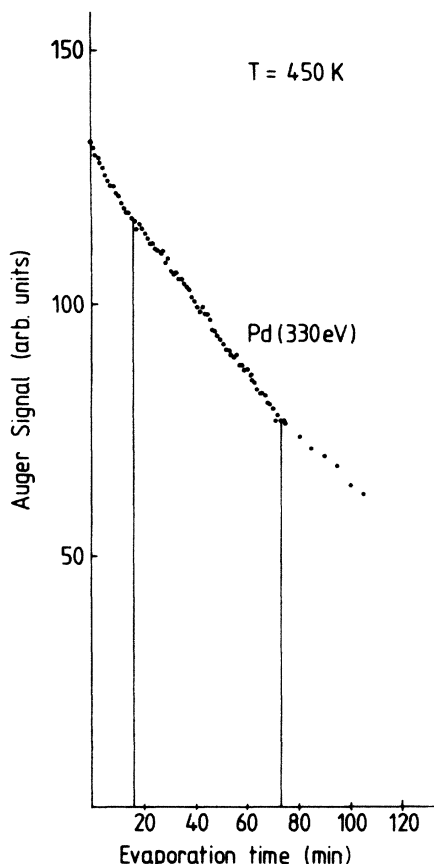


FIG. 2. A_s-t plot of the Pd MVV Auger signal for deposition of Fe onto the substrate at 450 K. The vertical lines mark the breaks in the curve.

in the literature a value for ψ , but we can obtain a rough estimate for ϕ by comparing the work necessary to separate two palladium atoms and two iron atoms. This gives $N_{12}=20$ atoms.

From the position of the first break in Fig. 2, the critical monolayer island size is reached at a coverage of about 0.5 monolayers. From the position of the bilayer break we find the scattering length in iron for electrons with a kinetic energy of 330 eV to be $\lambda=3.52\pm 0.05$ monolayers. This compares with a "universal curve" value of $\lambda=3.69$ monolayers.¹¹ Using this value of λ and the expressions given in Ref. 9 we can determine the coverage of an SM iron overlayer to within ± 0.05 monolayers from the decay of the palladium MVV Auger signal.

An implication of our interpretation of the high temperature A_s-t plot is that if we form an SM overlayer at low temperature, of coverage $\Theta < 0.5$ monolayers and anneal it, the overlayer will be transformed into monolayer platelets. On the other hand, if the initial SM overlayer has a coverage in the range $0.5 < \Theta < 2$ monolayers, then annealing will produce bilayer platelets. Carrying out these procedures resulted in different changes in the photoemission spectra. We take this as evidence supporting the above transformations on heating. For ease of discussion in the following text, we will refer to the substrate

maintained at room temperature or below as a "cold substrate" and the substrate maintained at 450 K as a "hot substrate."

In summary then, we can control the growth of iron on Pd(111) as follows. We can create an SM overlayer of any thickness by evaporating onto the cold substrate and measure the coverage to within ± 0.05 monolayers. We can create monolayer platelets by evaporating onto the hot substrate and interrupting the evaporation at a coverage $\Theta < 0.5$ monolayers or by forming an SM overlayer with this coverage on the cold substrate and heating. We must bear in mind that the overlayers formed by the different techniques may not have exactly the same properties. For example, the average platelet size could be different, and this may have a bearing on the photoemission results. In practice, during most evaporation runs we formed the flat monolayer or bilayer platelets by evaporating a suitable coverage onto the cold substrate and heating. This enabled us to rapidly contrast differences between an iron overlayer in an SM structure and a flat monolayer or bilayer structure. Note that, after heating, the sample was always cooled back down to liquid-nitrogen temperature before photoemission spectra were taken.

B. LEED results

Only $p(1\times 1)$ LEED patterns were observed at all iron coverages and temperatures. Variations in the quality of the LEED patterns, however, gave some insight into the overlayer structure. Palladium has a fcc structure with lattice constant 3.89 Å while below 1183 K; iron has a bcc structure with lattice constant 2.87 Å. The atomic diameter mismatch is thus 7.6%.

During evaporation onto the cold substrate, the LEED pattern began to noticeably degrade at about two monolayers. The loss of definition was by increase in spot size and background intensity indicating disorder due to variation in lattice constant. For an SM overlayer, this coverage would contain significant coverages in the third and fourth layers and the degradation of the LEED pattern suggests relaxation of the topmost iron layers towards the bulk bcc iron atomic diameter. Beyond this coverage, the LEED pattern degraded continuously. If, on the other hand, we formed a dense iron bilayer by evaporation onto the hot substrate, the quality of the LEED pattern was not noticeably different from that of the clean substrate. This indicates that the iron bilayer is well ordered and forms two atomic layers of an fcc lattice with a lattice constant identical to that of palladium. If we continued to evaporate onto this bilayer, the LEED pattern began to degrade almost immediately. The LEED results thus indicate that relaxation of the iron overlayer begins in the third layer.

C. PES results

Figure 3(a) shows the raw photoemission data recorded at 160-eV photon energy in the region of the iron 3s multiplet. The determination of the multiplet splitting (MS) of the iron levels is complicated, notably at low coverages, by the proximity of the palladium 4s feature at 88.1-eV

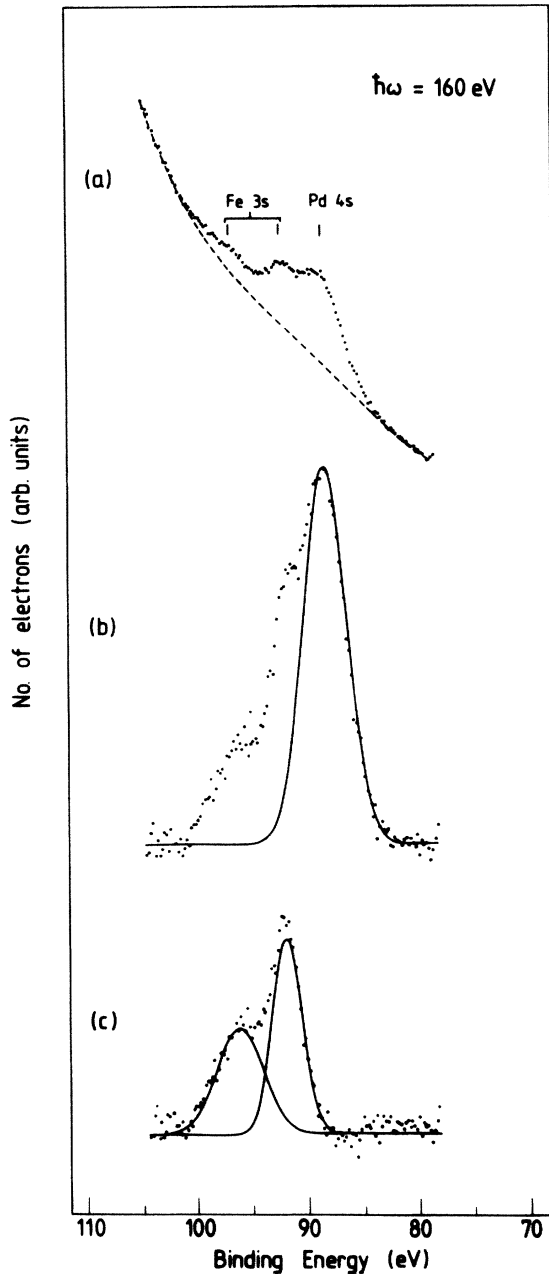


FIG. 3. Photoemission spectrum of Fe 3s and Pd 4s core levels from 0.4 monolayers Fe deposited onto the cold substrate. (a) Raw data treatment showing core levels and fitted background. (b) Data with background removed and Gaussian fitted to Pd 4s peak. (c) Data with Pd 4s peak removed and Gaussians fitted to Fe 3s spectrum.

binding energy and we adopted the following procedure. The secondary background, either side of the core features, we first fitted to a fifth-order polynomial. The spectrum with the background removed was then fitted to three Gaussians as shown in Figs. 3(b) and 3(c). It is shown that many-body, valence electron-core hole interactions give rise to asymmetric peak shapes.¹² To first order, however, this does not affect the MS and in conse-

quence was not considered in the analysis of the data which was limited by an inherent low signal-to-noise ratio.

Figure 4 shows the behavior of the iron 3s multiplet as iron is deposited onto the cold substrate, that is, in the SM mode. We have aligned the higher energy 3s peak and have not attempted to show any binding energy shifts which were small throughout the experiment. The iron 3s spectrum at coverage $\Theta=0.2$ monolayers appears as a single asymmetric peak without any indication of a doublet structure. We believe this is a result of the iron atoms existing in a variety of rather different local atomic arrangements and therefore exhibiting several local atomic arrangements and therefore exhibiting several values of the MS. This point is discussed more fully in Sec. IV.

At all coverages beyond $\Theta=0.2$ the doublet structure is apparent and the spectra have been analyzed on the assumption that there are only two 3s peaks. At $\Theta=0.4$, the MS is 4.6 ± 0.2 eV which corresponds within the error to the bulk iron value of 4.5 eV.¹³ As the thickness of the SM iron layer is increased, a decrease in the MS is ob-

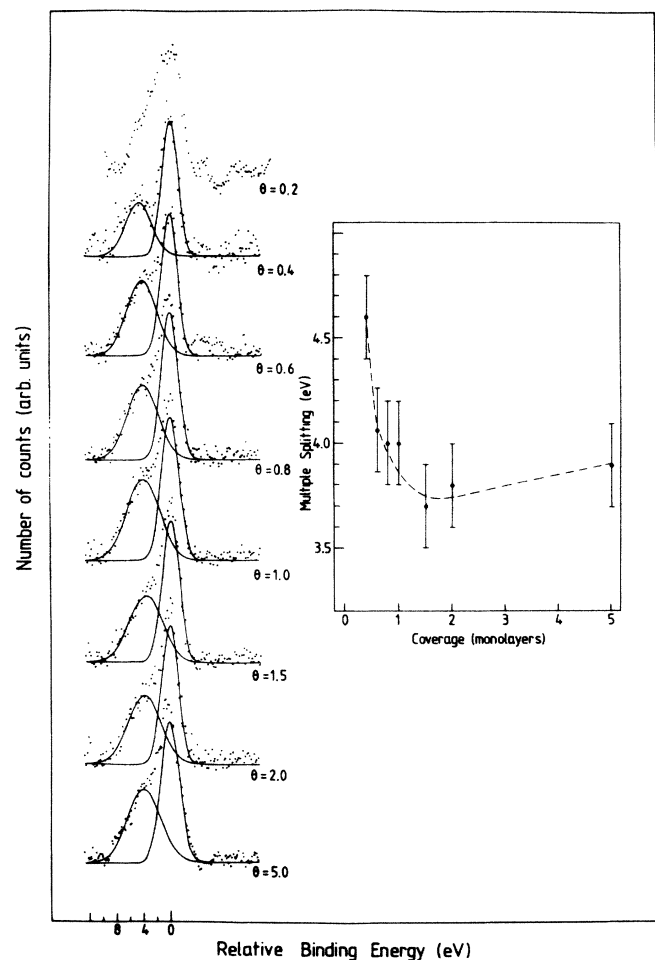


FIG. 4. Photoemission spectra of the Fe 3s core level as a function of thickness of the Fe film (in monolayers) deposited onto the cold substrate. Inset shows the MS plotted against coverage.

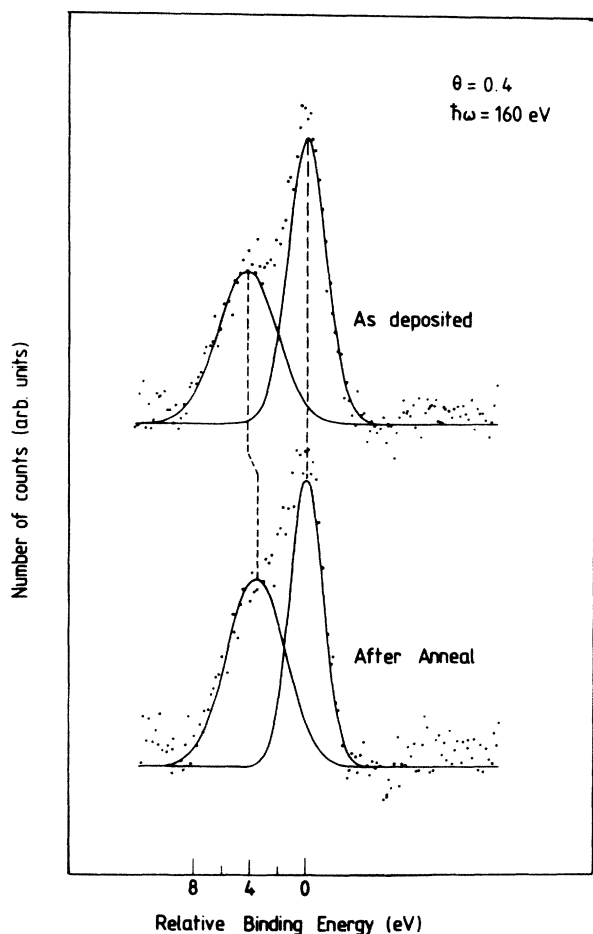


FIG. 5. Photoemission spectra of the Fe 3s core level from 0.4 monolayers of Fe deposited onto the cold substrate and then heated.

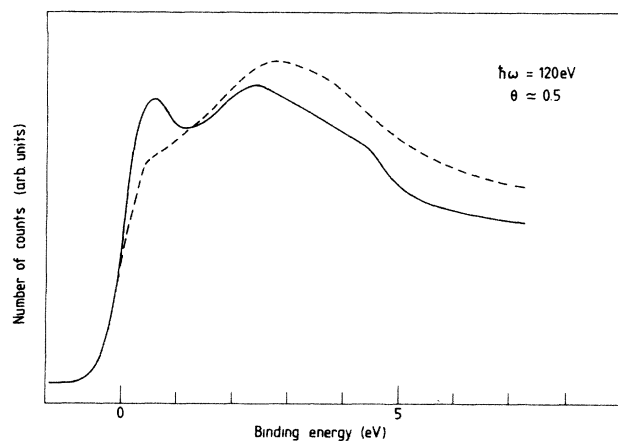


FIG. 6. Angle-integrated photoemission spectra of the valence-band region taken from an Fe film of thickness ≈ 0.5 monolayers. —, as deposited onto the cold substrate. — —, after heating. (Data reproduced from Ref. 8.)

served, a minimum value of 3.7 eV being found near 1.5 monolayers. Using the expressions of Barthes and Roland⁹ we estimate that this film has 52% of the iron atoms in the first layer and 29% in the second layer, the remainder being in the third and higher layers. This means that about 80% of the palladium surface is covered and about 60% of the first iron layer is covered by second layer. Thus, the majority of iron atoms have a coordination similar to that in a perfect bilayer. As the coverage is increased further, the MS appears to increase slowly, reaching 3.9 eV at 5 monolayers. The LEED results indicate that relaxation begins in the third layer, and as significant coverages are achieved in this and higher layers, we would expect the MS to tend towards the bulk ferromagnetic value of 4.5 eV.

Figure 5 shows the behavior of the iron 3s multiplet

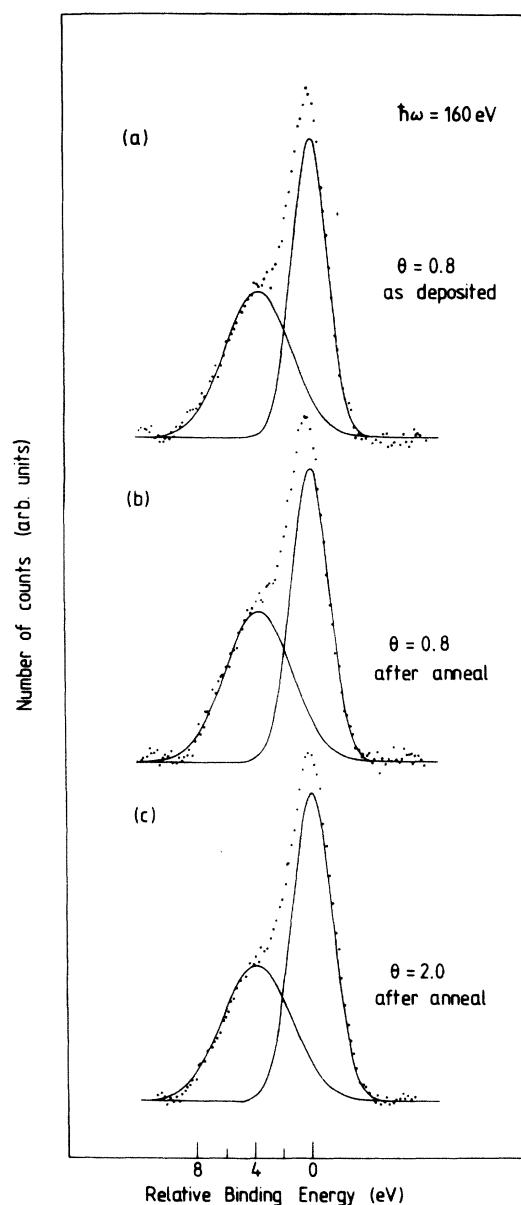


FIG. 7. Photoemission spectra of the Fe 3s core level. (a) 0.8 monolayers Fe deposited onto the cold substrate. (b) 0.8 monolayers Fe after annealing. (c) 2 monolayers Fe after annealing.

when an overlayer of $\Theta=0.4$ monolayers coverage is prepared on the cold substrate and annealed at 450 K. As stated earlier, this causes a structural transition from an SM arrangement to one consisting of flat monolayer platelets (hereafter referred to as an SM-M transition).

As can be seen from the figure the atomic rearrangement is accompanied by a reduction in the MS from 4.3 to 3.6 eV. The latter is the lowest value we observed for any iron overlayer and is 0.9 eV less than the value for the bulk. In an earlier measurement⁸ where the statistics were poorer, the weak shoulder could not be discerned and the spectrum appeared as a single peak. Figure 6 shows the angle integrated photoemission spectrum of the valence-band region before and after annealing. Since the photon energy, 120 eV, corresponds to the Cooper minimum for palladium 4*d* orbitals, the spectra are dominated by emission from the iron 3*d* levels. We note that there is a significant reduction in the density of states at the Fermi level on completion of the SM-M transition.

Figures 7(a) and 7(b) show the behavior of the iron 3*s* multiplet as 0.8 monolayers of iron are evaporated onto the cold substrate and then annealed. This results in a transition from an SM film to flat bilayer platelets (hereafter referred to as an SM-B transition). No significant change is observed in the MS which remains at around 3.7 eV. For comparison, a further 1.2 monolayers was evaporated onto the annealed iron film and the sample was reannealed. On completion of this procedure, the iron film should consist of a dense bilayer and it is seen that, apart from an improvement in statistics, the 3*s* spectrum obtained from this film [Fig. 7(c) is identical to that of the annealed 0.8 monolayer film, Fig. 7(b)].

The lack of change of the MS which characterizes the SM-B transition is in marked contrast to the change observed for the SM-M transition. It also contrasts with the behavior of the valence band. Figure 8 shows the valence band photoemission spectra taken at 120-eV photon energy for the 0.8 monolayer film before and after annealing. As with the lower coverage there is a significant reduction in the density of states at the Fermi level.

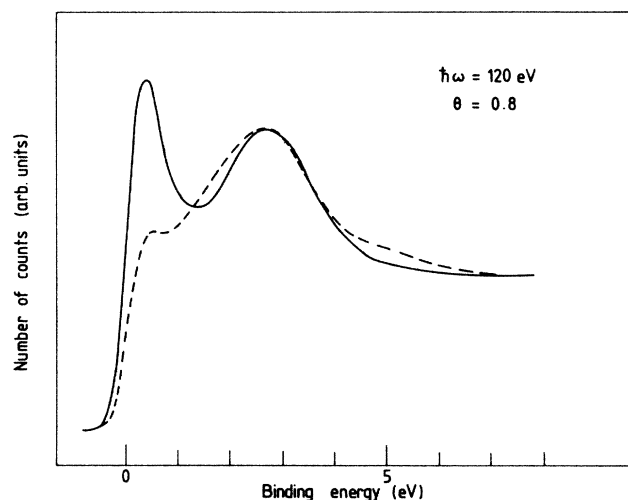


FIG. 8. Angle-resolved photoemission spectra of the valence band region from an 0.8 monolayer Fe film. —, A_S deposited film. - - -, after annealing.

IV. DISCUSSIONS

A. General considerations

It is well established that the splitting of core-level photoemission peaks from open-shell systems is due to the exchange interaction between the valence electrons and the *s* core electron left after the photoemission event.¹⁴ If the spin of the remaining *s* electron is aligned with that of the valence shell, the interaction results in a lower energy of the ion and thus a larger kinetic energy of the outgoing electron. Within the Hartree-Fock approximation the energy splitting is given¹⁵ by

$$\Delta E = \frac{2s+1}{2l+1} G^1(sl),$$

where *s* is the spin of the initial state and $G^1(sl)$ is the Slater integral for exchange between the *s* electron and the valence shell. The linear relationship between *s* and the MS of the iron 3*s* level has been verified in photoemission studies of the iron fluorides.¹⁶ The magnitude of the MS predicted by equation (1) however, is too large by a factor of 2. This discrepancy is due to intra-atomic correlation which has been shown to produce a constant factorial reduction of the MS for a range of 3*d* materials.¹⁴ Since we are dealing with a single element, we can assume that intra-atomic correlation simply provides an additional multiplication factor on the right-hand side of equation (1).

The magnitude of the MS in itinerant systems can be influenced by the majority spin correlation (MSC) effect described in Ref. 13. This effect is a result of the Pauli principle tending to separate spin-up itinerant *d* electrons from the core region in atoms which have been left in a high spin state after photoionization. Thus, if there is a change in the number of itinerant *d* electrons resulting from a structural reorganization of an iron overlayer, a concomitant change in the multiplet splitting may be due to MSC rather than a change of local moment. An increase in the itinerant character of an overlayer will tend to produce an increase in the MS. If we examine our 3*s* data for the SM-M transition (Fig. 5), we see that there is a large decrease in the MS accompanying the transition to flat monolayer platelets. It is hard to imagine that the patchy islanded structure in the SM overlayer has a more itinerant character than the flat monolayer structure formed after the transition, so we conclude that MSC is not a significant effect here. We will therefore assume that changes in the MS of the iron 3*s* core level reflect changes in the localized magnetic moment on the iron atoms.

B. 0.2 monolayer film

The iron 3*s* spectrum from the 0.2 monolayer film is a single asymmetric peak (Fig. 4). We believe this is due to the iron atoms existing in a variety of atomic arrangements, each characterized by a different local moment. Figure 9 shows a computer-generated lattice gas formed on an fcc(111) surface by an overlayer of thickness 0.2 monolayers, assuming insignificant surface diffusion. According to the plot, 33% of the overlayer atoms have

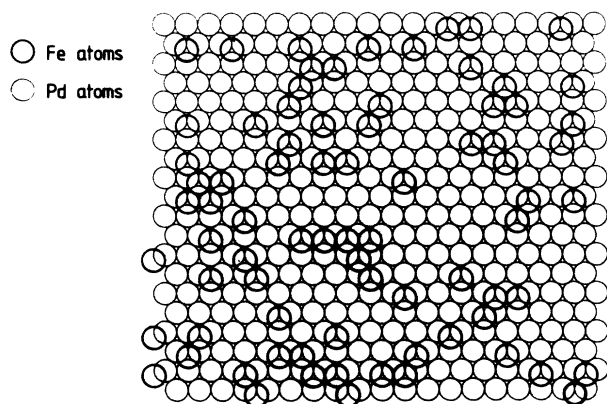


FIG. 9. Lattice gas of coverage 0.2 monolayers formed on the Pd(111) surface.

within the plane a zerofold coordination, 44% have a onefold coordination, 17% have a twofold coordination, and the remaining 6% are higher-fold coordinated. There is clearly dominant grouping. The resultant mixture of multiplet splittings would give the asymmetric hump observed. As the coverage increases, the overlayer rapidly becomes dominated by atoms with coordination greater than two and a single multiplet splitting becomes dominant.

C. 0.4 monolayer film

The 0.4 monolayer SM film shows a MS of 4.5 eV (Figs. 4 and 5) which is the value observed in bulk ferromagnetic iron¹³ and corresponds to a local moment of $2.3\mu_B$.¹⁷ This implies magnetic order in the film since, in an itinerant system, absence of magnetic order results in a reduced local moment. Moreover, neutron-diffraction studies of iron structures with antiferromagnetic order reveal a smaller local moment in these systems than in ferromagnetic iron.¹⁸ We conclude that the 0.4 monolayer SM film is ferromagnetic.

Some insight into the magnetic state of the overlayer after the SM-M transition can be gained by comparing our photoemission results with anomalous Hall effect measurements on iron films performed by Bergmann.⁷ As discussed in Ref. 8 we believe that Bergmann's films were islanded as were ours prepared on the cold substrate. Bergmann found that films greater than 0.5 monolayers thickness were ferromagnetic and that increasing the coverage from 0.52 to 0.7 monolayers increased the Curie temperature of the film from 10 to 20 K. Thus there is a correlation between the proportion of atoms in the second layer and the Curie temperature. Extrapolating this result backwards suggests that if there are no atoms in the second layer the film would be paramagnetic. The tendency of palladium to quench magnetic order in iron monolayers in contact with palladium has also been observed using Mössbauer spectroscopy.¹⁹

On annealing the 0.4 monolayer iron film, an overlayer of flat monolayer platelets is produced with every iron atom in contact with the palladium substrate. Bearing in mind the above discussion, we suggest this overlayer is

paramagnetic and the large decrease in the local moment after the SM-M transition is the result of a ferromagnetic-to-paramagnetic transition to the overlayer. This proposal is supported by the valence-band photoemission results (Fig. 6) which show a significant decrease in the density of states at the Fermi level after annealing. An itinerant system requires density of states at the Fermi level to support either ferromagnetic or antiferromagnetic order.²⁰ There is a significant contribution to the peak at the Fermi level from the $3d$ resonance of iron atoms on top of the monolayer. The large drop in this peak on annealing is consistent with our structural model. According to the calibration of Kowalczyk,¹⁶ the MS measured from the monolayer platelets corresponds to a local magnetic moment of $1.2\mu_B$. If our interpretation is correct, this is the true paramagnetic moment and is thus the lower limit of the instantaneous moment in condensed iron.

This paramagnetism is not a direct result of the low dimensionality of the film. The well-known result, that apart from an Ising system²¹ a two-dimensional film cannot support magnetic order above $T=0$, is due to singularity in the distribution function of spin waves at the long-wavelength limit. Since the photoemission event takes place on a time scale of the order of 10^{-15} sec, the fluctuations in magnetic moment produced by long-wavelength spin waves will be undetectable. Thus we believe the flat iron monolayer on Pd(111) to be a true dead layer incapable of supporting magnetic order at any temperature.

Another possible explanation for paramagnetism in the monolayer is that the band structure of a two-dimensional iron film may be unable to support magnetism. We rule this out since a smaller overlap of the iron $3d$ wave functions tends to increase the local moment. Thus calculations of the electronic structure of a two-dimensional iron film²² and one-dimensional iron chains²³ predict ferromagnetism with local moment of $3.4\mu_B$ and $3.3\mu_B$ respectively, compared to the bulk value of $2.3\mu_B$.

We conclude that the paramagnetism of the iron film is due to the interaction between the iron monolayer and the palladium substrate. The tendency for quenching of magnetic order at a palladium iron interface has also been observed by Hosoi *et al.*¹⁹ who noted a drastic lowering of the Curie temperature of an iron surface when it was coated with palladium. This behavior is in marked contrast to the behavior of isolated iron impurities in palladium which are characterized by a giant moment.⁵ A possible mechanism for the observed behavior of the iron monolayer could be a lowering of the iron $3d$ states due to bonding with the palladium $4d$ states due to their proximity in energy. As the iron $3d$ band is pulled progressively below the Fermi level and more of the minority spin band is filled, the spin polarization is reduced and will eventually collapse.

Prior to annealing, the ferromagnetic 0.4 monolayer iron film can be considered to be monolayer islands supporting a small number of atoms (6%) in the second layer. The implication of this is that if the paramagnetic flat monolayer structure, formed after annealing, is covered by a dilute lattice gas of iron atoms, the film will become fer-

romagnetic. Molecular bonding of an isolated iron atom to an iron monolayer will tend to stabilize a magnetic moment on the atom and its nearest neighbors, which in turn will tend to polarize a small region around it, and some critical coverage in the second layer the regions will overlap producing a ferromagnetic layer.

D. 0.8 monolayer film and the SM-B transition

Accompanying the SM-B transition there is a large decrease in the density of states at the Fermi level (Fig. 8) but no detectable change in the MS (Fig. 7), though a change of 0.2 eV or less would be undetectable. The magnetic state in the monolayer SM film is characterized by a small local moment and a high density of states at the Fermi level. We suggest that this film is antiferromagnetic for the following reasons. In itinerant systems, both ferromagnetic and antiferromagnetic order require a high density of states at the Fermi level but the time-averaged moment in the latter state is lower than in the former ($0.7\mu_B$ and $2.3\mu_B$, respectively). Moreover, fcc iron is antiferromagnetic and the iron overlayer forms at least two layers of an fcc structure before any relaxation towards the bcc lattice, so it is reasonable to suppose that at some coverage the film will pass through an antiferromagnetic phase. At a total coverage of 0.8 monolayers, the coverage in the first, second, and third iron layers is 0.55, 0.19, and 0.05 monolayers, respectively. This means that 35% of the first layer is covered by a second layer and 25% of the second layer is covered by a third layer, so a significant proportion of the fcc structure is in place. Our suggested magnetic structure in the 0.4- and 0.8-monolayer films imply a ferromagnetic-to-antiferromagnetic transition in the iron film as the coverage in the second layer increases. Judging by the rate at which the MS decreases between 0.4 and 0.6 monolayers, this transition is fairly sharp, and we estimate the critical coverage in the second to be around 0.2 monolayers. The proposed ferromagnetic-to-antiferromagnetic transition as the coverage in the second layer increases suggests a Ruderman-Kittel-Kasuya-Yosida (RKKY) type of interaction which tends to align moments parallel above some critical adatom separation but antiparallel below it.

After the SM-B transition the large decrease in the density of states at the Fermi level suggests that the overlayer has formed a dead layer. The small change in MS on going from a low-moment antiferromagnetic to a paramagnetic state would not be detectable. This behavior is puzzling since, in view of the above discussion, we would expect the film to remain antiferromagnetic as it became a perfect bilayer. Alternative magnetic probes such as Mössbauer spectroscopy would be of value.

Our results show the sensitivity of the magnetic state of iron to the local atomic coordination. Precise information on the detailed structure of a magnetic film is required in conjunction with magnetic measurements.

V. CONCLUSIONS

Photoelectron spectroscopy of the iron 3s core level and valence band has been used to study ultrathin iron overlayers on Pd(111) characterized by LEED and AES. The growth is perfectly epitaxial for two atomic layers, with relaxation beginning in the third layer. Marked changes in the Fe 3s spectra occur as a function of film thickness and heat treatment. We suggest the perfect iron monolayer is paramagnetic with an instantaneous local moment of $1.2\mu_B$. Small iron coverages (<0.2 monolayers) on top of this film induce ferromagnetic order with the bulk ferromagnetic moment of $2.3\mu_B$. Coverages in the range 1–2 layers, which have an fcc structure, may be antiferromagnetic. Coverages greater than 5 monolayers show a local moment approaching that of bulk iron.

ACKNOWLEDGMENTS

We gratefully acknowledge the support provided by The Science and Engineering Research Council (SERC), Daresbury Laboratory and the National Synchrotron Light Source (NSLS), Brookhaven National Laboratory. Essential technical support was provided by Mr. J. S. G. Taylor throughout these experiments. Beamline U14 at the NSLS was expertly maintained by M. Kelly. The work was supported by SERC Grant No. 61-09-04. One of us (C.B.) wishes to acknowledge the SERC for financial support. Brookhaven National Laboratory is supported by the United States Department of Energy under Contract No. DE-AC02-76Ch00016.

¹D. T. Pierce and H. C. Siegman Phys. Rev. B 9, 4035 (1974).

²Gerd Bergmann Phys. Today 32(8), 25 (1979).

³J. Tersoff and L. M. Falicov, Phys. Rev. B 52, 2959 (1982).

⁴E. Bergter, U. Gradmann, and R. Bergholz, Solid State Commun. 53, 565 (1985).

⁵A. M. Clogston, B. T. Matthias, M. Pettern, H. J. Williams, E. Corenzwit, and R. C. Sherwood, Phys. Rev. 125, 541 (1962).

⁶U. Gradmann and R. Bergholz, Phys. Rev. Lett. 52, 771 (1984).

⁷G. Bergmann, Phys. Rev. B 23, 3805 (1981).

⁸C. Binns, C. Norris, I. Lindau, M. L. Shek, B. Pate, P. M. Stefan, and W. E. Spicer, Solid State Commun. 43, 853 (1982).

⁹M-G. Barthes, and A. Rolland, Thin Solid Films 76, 45 (1981).

¹⁰S. A. Stoyanov and I. Markov, Surf. Sci. 116, 313 (1982).

¹¹M. P. Seah and W. A. Dench, Surf. Interface Anal. 1, 2 (1979).

¹²G. K. Wertheim and P. H. Citrin, in *Photoemission in Solids I*, edited by M. Cardena and L. Ley (Springer, Berlin, 1978), p. 197.

¹³D. J. Joyner, O. Johnson, and D. M. Hercules, J. Phys. F 10, 169 (1980).

¹⁴D. A. Shirley, in *Photoemission in Solids I*, edited by M. Cardona and L. Ley (Springer, Berlin, 1978), p. 165.

¹⁵J. A. Van Vleck, Phys. Rev. 45, 405 (1934).

¹⁶S. P. Kowalczyk, Ph.D thesis, University of California at Berkeley, LBL Report No. 4319, 1976 (unpublished).

¹⁷C. Kittel, *Elementary Solid State Physics* (Wiley, New York,

- 1962), p. 276.
- ¹⁸S. C. Abrahams, L. Guttman, and J. S. Kasper, *Phys. Rev.* **127**, 2052 (1962).
- ¹⁹N. Hosoito, T. Shinjo, and T. Takada, *J. Phys. Soc. Jpn.* **50**, 1903 (1981).
- ²⁰G. C. Fletcher and R. P. Addis, *J. Phys. F* **4**, 1951 (1974).
- ²¹L. Onsager, *Phys. Rev.* **65**, 17 (1944).
- ²²J. Noffke and L. Fritsche, *J. Phys. C* **14**, 89 (1981).
- ²³M. Weinert and A. J. Freeman, *J. Magn. Magn. Mater.* **38**, 23 (1983).